Supplementary material

Ultra-small CoO_x/GO catalyst supported on ITO glass by electrochemical post-treatment of redox-active infinite coordination polymer: a portable reactor for real-time monitoring catalytical oxidative degradation of colored wastewater

Xinrui You,[a,b] Chunyu Huang,[a,b] Wei Huang,[a,b] Guoyue Shi,[c] Jingjing Deng*[a,b] and Tianshu Zhou*[a,b]

[a]*School of Ecological and Environmental Sciences, Shanghai Key Lab for Urban Ecological Process and Eco-Restoration, East China Normal University, 500 Dongchuan Road, Shanghai 200241, China.*

[b]*Institute of Eco-Chongming, 3663 Zhongshan Road, Shanghai 200062, China.*

[c]*Department of Chemistry, East China Normal University, 500 Dongchuan Road, Shanghai 200241, China.*

* Corresponding Authors: E-mail: jjdeng@des.ecnu.edu.cn, tszhou@des.ecnu.edu.cn

Fax: +86-21-54341277, Tel: +86-21-54341277

Table S1. Comparison of synthesis methods for cobalt oxide.

Samples	Synthesis method		Reaction temperature $_{max}$ (°C)	Reaction time (h)		Sample size (nm)
	Step 1	Step 2		Step 1	Step 2	
CoO/ MWCNTs[1]	Spray pyrolysis	–	1000	–	–	40 ± 10
Co_3O_4[2]	Hydrothermal	–	500	8	–	500
Co_3O_4@PFR[3]	Hydrothermal	–	160	6.33	–	60
Co_3O_4[4]	Pulsed laser deposition	–	250	25 ns	–	50
Co_3O_4@N-C[5]	Hydrothermal	Thermal decomposition	800	96	12	20
CoO_x/CPC[6]	Hydrothermal	Thermal decomposition	500	26	24	100
Mesoporous Co_3O_4[7]	Ball milling	Calcination	400	1	27	10-14
Co_3O_4[8]	Solvothermal	Calcination	700	3	12	32.3
Co_3O_4 NPs/TNWs[9]	Hydrothermal	Calcination	450	30	8	22 ± 3
Co_3O_4[10]	Mixing	Calcination	400	–	2	48
Co_3O_4[10]	Calcination	Electron beam deposition	400	2	2	27
Co_3O_4[10]	Sol-gel method	Heat treatment	400	0.5	2	20
Co_3O_4[10]	Electroless deposition	Heat treatment	400	–	2	38
CoO_x (This work)	Mixing	Electrochemical post-treatment	Room temperature	0.08 (5 min)	0.28 (16.7 min)	1.42 ± 0.34

Table S2. Mass ratio of O and Co in the TEM-EDS of CoO_x.

Spectra	Instate	O	Co	Total
1	Yes	25.42	74.58	100.00
2	Yes	25.13	74.87	100.00
3	Yes	25.59	74.41	100.00
4	Yes	25.18	74.82	100.00
5	Yes	25.31	74.69	100.00
Average		25.32	74.68	100.00

Table S3. The pseudo-first-order rate constants of MB degradation by CoO_x/GO catalyst activated PMS under various conditions (C_{MB} = 20 mg/ L).

Catalyst (mg)	PMS (mmol L^{-1})	Temp. (^oC)	pH	Additive	k_1 (min^{-1})
0.1	0.5	60	7.0	–	0.487
0.3	0.5	60	7.0	–	0.738
0.5	0.5	60	7.0	–	0.764
0.6	0.5	60	7.0	–	0.784
0.8	0.5	60	7.0	–	0.828
0.5	0.25	60	7.0	–	0.353
0.5	0.5	60	7.0	–	0.766
0.5	1.0	60	7.0	–	1.565
0.5	2.0	60	7.0	–	2.140
0.5	0.5	60	3.0	–	0.351
0.5	0.5	60	5.0	–	0.731
0.5	0.5	60	9.0	–	0.742
0.5	0.5	60	11.0	–	0.279
0.5	0.5	30	7.0	–	0.068
0.5	0.5	45	7.0	–	0.231
0.5	0.5	60	7.0	–	0.766
0.5	0.5	75	7.0	–	1.440
0.5	0.5	60	7.0	0.5 g L^{-1} $NaNO_3$	0.847
0.5	0.5	60	7.0	0.5 g L^{-1} NaCl	0.183
0.5	0.5	60	7.0	0.5 g L^{-1} $NaHCO_3$	0.080
0.5	0.5	60	7.0	0.5 mol L^{-1} TBA	0.699
0.5	0.5	60	7.0	0.5 mol L^{-1} MeOH	0.141
0.5	0.5	60	7.0	2 mol L^{-1} TBA	0.273
0.5	0.5	60	7.0	2 mol L^{-1} MeOH	0.025

Table S4. Activation energy values for dye degradation using PMS activated by various cobalt-based catalysts.

Catalysts	Dyes	Ea (kJ/mol)
MCC[11]	Amaranth	64.5
$CoMoO_4$[12]	Methylene blue	69.89
Co-Mn LDH[13]	Acid orange G	72.29
CoCNF[14]	Amaranth	70.4
CoO_x/GO (This work)	Methylene blue	60.78

Table S5. Comparison of various catalysts for catalytical oxidative degradation of MB by activation of PMS.

Catalyst	Dose of catalyst (mg)	Dose of PMS (mg)	Amount of MB (μg)	Degradation efficiency (%)	Degradation time
Co_3O_4 by PLD[4]	1.2	7.68	100	75	5 min (25 °C)
Co_3O_4 NPs/TNWs[9]	0.75	0.23	15	100	10 min (None)
Co_3O_4 powder[10]	0.3	1.47	15	59.5	10 min (25 °C)
Co_3O_4[15]	3.22	0.31	32	95.7	90 min (None)
Co_2O_3[15]	3.32	0.31	32	88.5	90 min (None)
CoO[15]	3.00	0.31	32	98.5	90 min (None)
Co_3O_4 /Graphene[16]	0.3	1.47	15	84.8	10 min (25 °C)
Co_3O_4/CNFs[17]	0.2	3.07	373	100	30 min (None)
CoPc/CFs[18]	4.00	0.62	18.7	48	10 min (50 °C)
Co/ACFs[19]	4.00	0.62	18.7	100	35 min (25 °C)
Co/N-CNTs[20]	1.00	2.00	100	100	2.5 min (None)
CoO_x (This work)	0.3	0.31	40	92.3	6.7 min (60 °C)
CoO_x /GO (This work)	0.5	0.31	40	100	6.7 min (60 °C)

Table S6. Catalytical oxidative degradation of MB and three colored wastewater samples.

Source of wastewater	Dose of catalyst (mg)	Dose of PMS (mmol L^{-1})	Degradation temperature (°C)	Degradation efficiency after 2 min by HPLC(%)	TOC (mg L^{-1})	TOC removal efficiency (%)
MB	0.5	0.5	60	99.90	39.1	80.64
Textile-1	0.5	9.3	60	98.66	725.5	71.95
Textile-2	0.5	3.5	60	98.99	278.1	74.94
Cosmetic	0.5	4.2	60	98.59	324.5	80.40

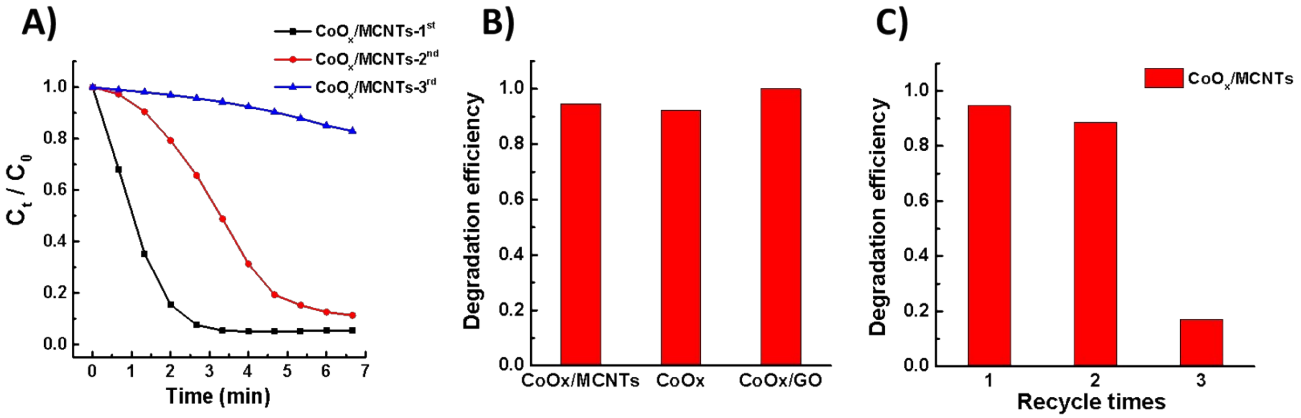

Fig. S1. (A) Degradation efficiency of MB (2.0 mL, 20 mg L^{-1}) in the presence of PMS (50 µL, 0.02 mol L^{-1}) and CoO_x/MCNTs nanocatalysts at different time intervals; (B) Degradation efficiency of MB (2.0 mL, 20 mg L^{-1}) with presence of same amount of nanocatalysts CoO_x/MCNTs (7/5), CoO_x, CoO_x/GO (7/5) supported on ITO glass after 6.7 min for the first run; (C) Recyclability of CoO_x/MCNTs (7/5) nanocatalyst supported on the ITO glass for degradation of MB.

Firstly, the conductive multi-walled carbon nanotubes (MCNTs) were mixed with Co-ICP and the catalytic activity of as-formed CoO_x/MCNTs nanocomposites towards the oxidation of MB by PMS was investigated. As demonstrated in Fig. S1A, B, within 6.7 min, 94.7 % MB (2.0 mL, 20 mg L^{-1}) could be degraded by PMS with the presence of CoO_x/MCNTs nanocatalysts, which was higher than that of the CoO_x NPs (92.3%), but lower than CoOx/GO nanocatalyst (100%). The stability of CoO_x/MCNTs nanocatalyst supported on ITO glass was also tested (Fig. S1C). After the 3rd run, the degradation efficiency was decreased to 14.9%, which was much lower than CoO_x/GO nanocatalyst (100%) (Fig. 7). The superiority of CoO_x/GO nanocatalyst may ascribe to the fact that two-dimensional structure of GO make it easily accessible for the deposition of CoO_x and increased the

robustness of the catalysts on ITO glass and their extraordinary adsorption capacity significantly promoted the dyes to accumulate on the surface of the catalyst and approached to the active oxidants. Consequently, GO was chosen as a matrix and mixed with Co-ICP as a precursor to obtain CoO_x/GO nanocatalyst supported on ITO glass for catalytical oxidative degradation of colored wastewater.

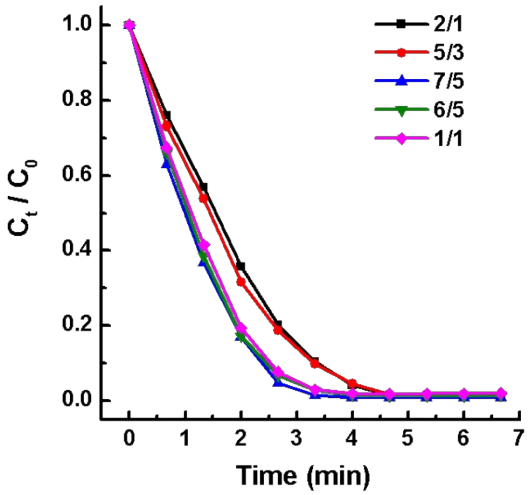

Fig. S2. Effect of different mass ratio of Co-ICPs to GO (2/1, 5/3, 7/5, 6/5 and 1/1) on the degradation of MB (Condition: C_{MB} = 20 mg L^{-1}; CoO_x/GO = 0.5 mg; PMS = 0.5 mmol L^{-1}; pH = 7.0; T = 60 °C).

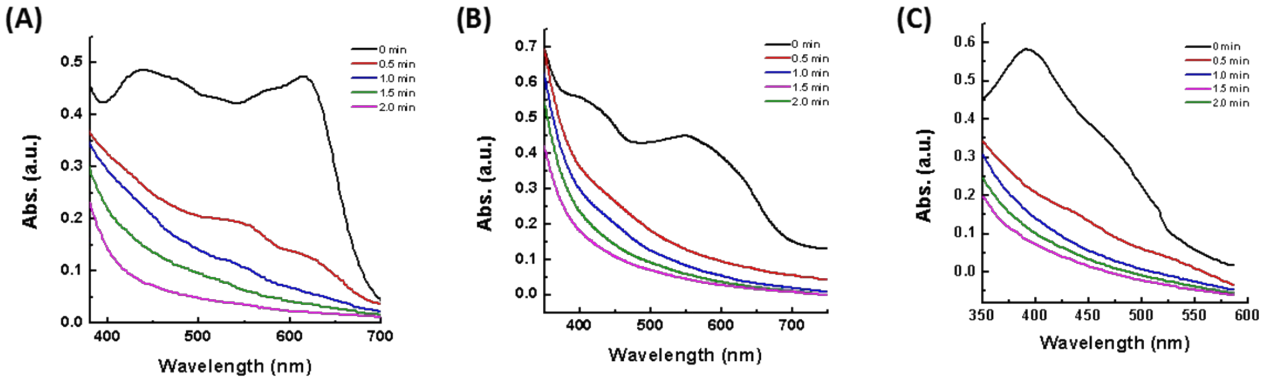

Fig. S3. UV-vis spectra of 2.0 mL wastewater textile-1 (A), textile-2 (B) and cosmetic (C) in reactor constructed by ITO glass with CoO_x/GO catalyst supported on. UV-vis spectra were consecutively recorded every 0.5 min shortly after the addition of PMS (9.3 mmol L^{-1} for textile-1, 3.5 mmol L^{-1} for textile-2, 4.2 mmol L^{-1} for cosmetic) at 60 °C.

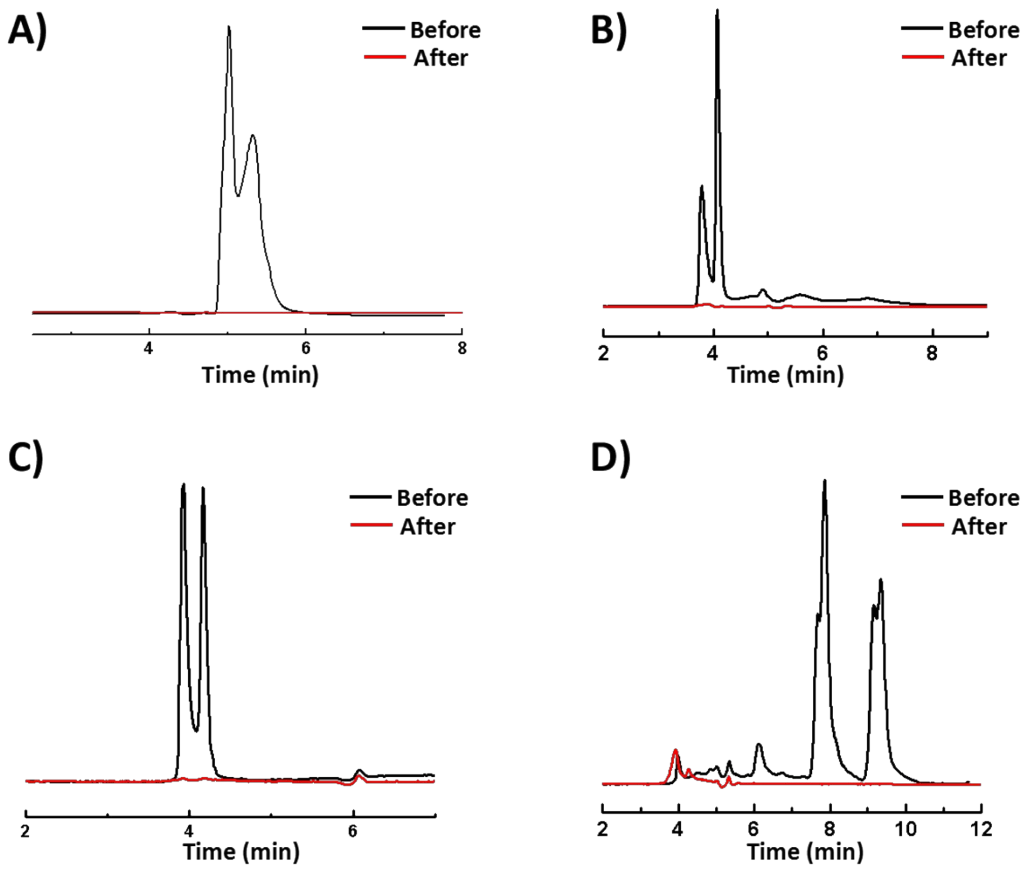

Fig. S4. Chromatogram of 2.0 mL MB (20 mg L^{-1}) (A), wastewater textile-1 (B), textile-2 (C) and cosmetic (D) in our reactor before (black curve) and 2 min after (red curve) the addition of PMS (0.5 mmol L^{-1} for MB, 9.3 mmol L^{-1} for textile-1, 3.5 mmol L^{-1} for textile-2 and 4.2 mmol L^{-1} for cosmetic) at 60 °C.

References

1. F. Lupo, R. Kamalakaran and A. Gulino, Viable route for cobalt oxide-carbon nanocomposites, *J. Phys. Chem. C*, 2009, **113**, 15533-15537.
2. X. Xiao, X. Liu, H. Zhao, D. Chen, F. Liu, J. Xiang, Z. Hu and Y. Li, Facile shape control of Co_3O_4 and the effect of the crystal plane on electrochemical performance, *Adv. Mater.*, 2012, **24**, 5762-5766.
3. J. Ma, W. Liu, S. Zhang and Y. Zhao, Co_3O_4@PFR cube-like core-shell nanocomposite prepared via a facile one-step hydrothermal approach, *J. Nanopart. Res.*, 2011, **13**, 1219-1228.
4. T. Warang, N. Patel, A. Santini, N. Bazzanella, A. Kale and A. Miotello, Pulsed laser deposition of Co_3O_4 nanoparticles assembled coating: Role of substrate temperature to tailor disordered to crystalline phase and related photocatalytic activity in degradation of methylene blue, *Appl. Catal. A: Gen.*, 2012, **423**, 21-27.
5. G. Zhang, C. Li, J. Liu, L. Zhou, R. Liu, X. Han, H. Huang, H. Hu, Y. Liu and Z. Kang, One-step conversion from metal-organic frameworks to Co_3O_4@N-doped carbon nanocomposites towards highly efficient oxygen reduction catalysts, *J. Mater. Chem. A*, 2014, **2**, 8184-8189.
6. W. Y. Choi, D. K. Lee, H.-T. Kim, J. W. Choi and J. W. Lee, Cobalt oxide-porous carbon composite derived from CO_2 for the enhanced performance of lithium-ion battery, *J. CO_2 Util.*, 2019, **30**, 28-37.
7. J. Liu, H. Cheng, J. Bao, P. Zhang, M. Liu, Y. Leng, Z. Zhang, R. Tao, J. Liu, Z. Zhao and S. Dai, Aluminum hydroxide-mediated synthesis of mesoporous metal oxides by a mechanochemical nanocasting strategy, *J. Mater. Chem. A*, 2019, **7**, 22977-22985.
8. Y. Cai, J. Xu, Y. Guo and J. Liu, Ultrathin, polycrystalline, two-dimensional Co_3O_4 for low-temperature CO oxidation, *ACS Catal.*, 2019, **9**, 2558-2567.
9. Z. Chen, S. Chen, Y. Li, X. Si, J. Huang, S. Massey and G. Chen, A recyclable and highly active Co_3O_4 nanoparticles/titanate nanowire catalyst for organic dyes degradation with peroxymonosulfate, *Mater. Res. Bull.*, 2014, **57**, 170-176.
10. T. Warang, N. Patel, R. Fernandes, N. Bazzanella and A. Miotello, Co_3O_4 nanoparticles

assembled coatings synthesized by different techniques for photo-degradation of methylene blue dye, *Appl. Catal. B: Environ*., 2013, **132**, 204-211.

11. K.-Y. A. Lin, Y.-C. Chen and C.-F. Huang, Magnetic carbon-supported cobalt prepared from one-step carbonization of hexacyanocobaltate as an efficient and recyclable catalyst for activating oxone, *Sep. Purif. Technol.*, 2016, **170**, 173-182.
12. Y. Fan, W. Ma, J. He and Y. Du, $CoMoO_4$ as a novel heterogeneous catalyst of peroxymonosulfate activation for the degradation of organic dyes, *RSC Adv.*, 2017, **7**, 36193-36200.
13. X. Zhao, C. Niu, L. Zhang, H. Guo, X. Wen, C. Liang and G. Zeng, Co-Mn layered double hydroxide as an effective heterogeneous catalyst for degradation of organic dyes by activation of peroxymonosulfate, *Chemosphere*, 2018, **204**, 11-21.
14. K.-Y. A. Lin, J.-T. Lin, X.-Y. Lu, C. Hung and Y.-F. Lin, Electrospun magnetic cobalt-embedded carbon nanofiber as a heterogeneous catalyst for activation of oxone for degradation of Amaranth dye, *J. Colloid Interface Sci.*, 2017, **505**, 728-735.
15. B. Zhang, Y. Zhang, W. Xiang, Y. Teng and Y. Ynag, Comparison of the catalytic performances of different commercial cobalt oxides for peroxymonosulfate activation during dye degradation, *Chem. Res. Chin. Univ.*, 2017, **33**, 822-827.
16. H. Sun, S. Liu, G. Zhou, H. M. Ang, M. O. Tadé and S. Wang, Reduced graphene oxide for catalytic oxidation of aqueous organic pollutants, *ACS Appl. Mat. Interfaces*, 2012, **4**, 5466-5471.
17. B.-T. Zhang, Y. Zhang and Y. Teng, Electrospun magnetic cobalt-carbon nanofiber composites with axis-sheath structure for efficient peroxymonosulfate activation, *Appl. Surf. Sci.*, 2018, **452**, 443-450.
18. Z. Huang, Y. Yao, J. Lu, C. Chen, W. Lu, S. Huang and W. Chen, The consortium of heterogeneous cobalt phthalocyanine catalyst and bicarbonate ion as a novel platform for contaminants elimination based on peroxymonosulfate activation, *J. Hazard. Mater.*, 2016, **301**, 214-221.
19. Z. Huang, H. Bao, Y. Yao, J. Lu, W. Lu and W. Chen, Key role of activated carbon fibers in enhanced decomposition of pollutants using heterogeneous

cobalt/peroxymonosulfate system, *J. Chem. Technol. Biotechnol.*, 2016, **91**, 1257-1265.

20. M. Chen, L. Zhu, Y. Zhang, J. Zou and H. Tang, Cobalt particles encapsulated and nitrogen-doped bamboo-like carbon nanotubes as a catalytic and adsorptive bifunctional material for efficient removal of organic pollutants from wastewater, *J. Environ. Chem. Eng.*, 2017, **5**, 5322-5330.